Article

Not peer-reviewed version

Shock Wave Structure in a Monatomic Gas Mix with Rydberg Atoms

A. Markhotok *

Posted Date: 8 May 2026

doi: 10.20944/preprints202605.0506.v1

Keywords: supersonic plasma dynamics; shock waves; shock structure

 doi:10.20944/preprints202605.0506.v1

Article

Shock Wave Structure in a Monatomic Gas Mix with Rydberg Atoms

A. Markhotok

Physics Department, Old Dominion University, Norfolk, VA 23529 USA; anavovkmarh@gmail.com

Abstract

The effect of atom size on the shock wave structure in a binary monatomic gas mix with Rydberg atoms has been investigated. The problem was solved numerically using the system of hydrodynamic equations in Argon gas, for the atom size ratios between 2 and 100, T = 1500 K, and the density between 10^{17} and 10^{20} m^{-3}. It was found that the presence of larger size atoms in the mix results in the shock front splitting that is on the order of mean free path for this component. The results can be of interest in supersonic plasma dynamics and in astrophysics studying shock waves in the environments where high-n Rydberg states are present.

Keywords: supersonic plasma dynamics; shock waves; shock structure

I. Introduction

The shock wave front represents a thin transitional layer separating gases in two states of thermodynamic equilibrium. In an atomic gas, this non-equilibrium area is formed by dissipative processes mostly mediated by collisions, in which viscosity and heat conduction play a dominant role, and in the presence of molecules the relaxation of internal degrees of freedom contribute additionally. Typical structure of a simple shock front represents a steep gradient in the gas parameters and their distribution is obtained from the solution of gas dynamic Euler equations.

The specific structure of the transitional layer across the shock is determined by the properties of the medium through which it propagates, thus additionally serving as a tool for probing various types of environments. In the simplest case of a shock in a uniform ideal gas, the hydrodynamic equations allow a discontinuous solution in which the shocked gas variables, including the entropy, experience an instantaneous jump, and therefore the shock front width is zero. Change in the entropy assumes dissipation, so a more realistic picture would include energy dumping mechanisms. Among them are the viscosity causing scattering of the directed energy of the shock into kinetic energy of random motion, and the heat conduction mediating redistribution of the pressure. When they are taken into account, the solution of hydrodynamic equations features the shock front of a final width on the order of a few mean free paths. In stronger shocks, the transitional layer width scales inversely proportionally to the Mach number and becomes very thin as the Mach number tends to infinity. In molecular gases behaving essentially non-ideally, additional degrees of freedom, such as rotations, vibrations, dissociation, electronic excitation and ionization, etc., significantly delay the establishment of equilibrium in the shocked gas. Given considerable variation in the relaxation times for the kinetical processes and in specific gases, the shock front widths can differ by an order of magnitude. Known for sharp dependence on the sort of gas, and sometimes within very narrow intervals of gas parameters, the contributions can result in the front widths of up to tens of mean free path lengths and more [1].

Structurally more complicated transitional layers across the shock are known to develop in binary gas mixes in which the molecular masses are different. In the process of diffusion between the components induced by the shock, lighter particles (of mass m_1) are pulled ahead of the heavy ones (mass m_2). The resulting component separation across the shock is proportional to the mean free path

 doi:10.20944/preprints202605.0506.v1

l, and it scales with the mass ratio as $l(m_2/m_1)^{1/2}$. The separation sharpness tends to increase when masses differ appreciably [2].

In plasma environments, such as gas discharges and interstellar or gaseous star media, the presence of charged particles gives rise to their separation after a passage through a shock wave. Since the heated ion velocity in the flow is comparable to the shock speed, the ions cannot move far ahead of the shock from the compressed area. However lighter hot electrons whose velocity is proportional to $(m_i/m_e)^{1/2}$, can easily reach the gas ahead of the shock. The resulting charge separation, with electrons located ahead of the ions, forms the preheating layer in front of the shock in which the electron temperature is sharply increased compared to the rest. During the relaxation, the component temperatures eventually equilibrate in collisions. However, because of large difference in the masses, very slow energy exchange between the components results in the relaxation zone of appreciable width. With the electron heat conduction taken into account, the thickness of the preheating layer ahead of the shock becomes comparable to the thickness of the relaxation layer behind it. The thickness scales with the ion mean free path l_i and the mass ratio as $l_i(m_i/m_e)^{1/2}$ and increases rapidly with the shock intensity [1].

Another type of the structure forms when a shock wave interacts with a sharp or an extended boundary separating two gases of different acoustic impedances [3–7]. As the result of refraction at the interface, the shock front experiences strong distortions, as for ex. described in [8,9], or when the shock reflections are involved [10]. The shock front modification is subsequently followed with the change in shock intensity and re-distribution of the gas parameters behind it, eventually resulting in the collapse of the gas volume involved in the interaction.

In further study on this topic, it would be interesting to see if the atom size could be another factor able to modify the shock structure. For this, a monatomic gas mix consisting of atoms with different sizes but of equal masses will be considered. Alternatively, a molecular gas mix consisting of two non-reacting chemically different components with large molecular size difference but with their masses being reasonably close, is another possibility to consider. While the size and mass factors can also be combined, for the size effect to be at least visible rather than canceled, the molecule of a larger size should have a smaller mass and vice versa. Even though it is possible in general, in most cases of substantial size difference it will not be the case, and therefore considering species that are different only chemically is rather impractical. In addition, molecular gases perturbed by the shock feature significant delays in establishment of thermodynamic equilibrium, and therefore possible overlapping with their contributions could obscure the studied effect.

Monatomic gases having a portion of its atoms excited to Rydberg state while others stay in the ground state, appear to be better candidates to include in the model as the atoms have equal masses and therefore allow investigation of the size effect exactly. Rydberg atoms are characterized by highly excited electronic states, for which at least one of the outer electrons has a large principal quantum number, up to n = 150–200. Therefore, the atom's most remarkable property is the extremely large electron orbit, with the wavefunction extension scaling as ~ n^2. For the states with low orbital quantum number l, the electron orbit is significantly eccentric making its charge distribution skewed. In this case, most of the time the electron spends on one side, at a larger distance from the core, where it slows down. This determines such remarkable atomic properties as large electric dipole moment, a high polarizability and as a consequence, high sensitivity to electric fields, including the fields of neighboring atoms [11]. An atom's electron can be sent to a Rydberg state by laser excitation, via electron scattering in collisions with other atoms or electrons, or via charge exchange mechanism. In laboratory plasmas, Rydberg atoms are commonly formed in the process of recombination of electrons and positive ions. The low energy recombination typically results in quite stable Rydberg atoms, while recombination of electrons and positive ions with high kinetic energy often form autoionizing Rydberg states [12].

Rydberg plasmas can be obtained in ultracold environments by photo-excitation of ultracold atoms to the levels below or above an ionization threshold. Considering bound states, plasma with ultracold Rydberg atoms is commonly formed via collisions between Rydberg atoms or three-body

 doi:10.20944/preprints202605.0506.v1

recombination. The so called "Zero Kinetic Energy" (ZEKE) Rydberg states, which are high angular momentum and high magnetic quantum number excited states, can be formed by laser excitation in the presence of electric fields, with the fields also capable of controlling the atom's lifetimes [13]. In ultracold gases, ultralong-range Rydberg molecules are formed by coupling of an excited Rydberg atom and a ground-state atom via low-energy elastic electron scattering [14], via coupling of electronic and nuclear spins and the fine and hyperfine structure of several atoms [15], or manipulation of these molecules by external fields [16]. The so called Rydberg polarons, the giant polyatomic molecules made of hundreds to thousands of atoms, are formed via electron mediating interactions of the Rydberg atom with several ground-state atoms through an additional spin coupling of the Rydberg states of a multivalent atom, or via the long-range spin entanglement and remote spin flip. Based on those mechanisms, the possibility for long-lived metastable states of heteronuclear (Hg*Rb) and homonuclear (Hg*Hg) molecules as resonances above the dissociation threshold was discussed in [14].

When considering shock waves in such environments, Rydberg atom stability with lifetimes comparable to the relaxation time in the compressed gas, i.e. at least on the level of hundreds *μs* to *ms*, is the basic requirement. Possessing very large electric dipole moment for the electron, when the perturbation to the electronic energy state during the collision exceeds the ionization potential, the atoms can be easily ionized. Seemingly being fragile and prone to quick decay back to the ground state, Rydberg atoms are actually found to be surprisingly stable and quite abundant in various environments. In space, Rydberg states are produced at very low densities, under the conditions of dynamic equilibrium between photoionization by hot stars and recombination with electrons. The newly accepted electron in a very high n state, during its gradual transitions down to the ground state, produces a sequence of recombination spectral lines by which the atoms are identified. Because of extremely small separations between neighboring Rydberg states, the radiation frequency is in the range of radio waves [17]. In 1964, such radio recombination lines were first detected by Russian radio astronomers, thus confirming the existence of stable Rydberg atoms of hydrogen, helium and carbon in space [18].

Due to specific collisional exchange mechanisms, the lifetimes of high n states via decay by spontaneous emission can be very long, typically on the order of tens to hundreds *mks*, and under special circumstances can be quite long, up to 10 *ms*, depending on Rydberg atom density in the mix. For ex., in the study [19] the authors found that in the absence of high field gradients, high-n Rydberg states exhibited stability, with lifetimes of around 30 *mks* (*s*-state in Na, $n = 30$). It was shown there that theoretically the lifetimes scale ~ n^{-3}, and stronger dependence ~ $n^{-4.5}$ was observed experimentally. The lifetimes were also found dependent on angular momentum numbers for the state, where for *p*-state it is typically longer, compared to *f*- and *d*- states for which it is shorter. In the plasma of discharges, in the region of cathode fall-negative glow, highly accelerated electrons result in atom ionization, while the positive column, where the electrons are slowed down, is the place where the bulk of Rydberg atoms form. In the presence of charge flow in the region, the atoms become stabilized by collisionally induced (*nlm*)-mixing of states and by removal of charge by charge transfer. Because of poor coupling of Rydberg states with ionization continuum in the area, Rydberg gas remains stable as long as it is conducting electric current.

In molecular gases of H_2, D_2, N_2, and CO, the researchers observed high-Rydberg states that were stable with respect to predissociation and autoionization, and had sufficiently long radiative lifetimes of the order of 100 μs [20]. There is an evidence of longer lifetimes, > 0.3 *ms*, in strongly-coupled molecular Rydberg plasma generated by excitation of nitric oxide in the high-density region of a supersonic jet expansion, in the broad range of excitation energies from threshold down to Rydberg states as low as $n = 19$ [21]. The lifetimes of around 0.5 *ms* were observed under ultra-cold conditions, in a plasma of para-difluorobenzene molecules obtained in strong collisional cooling inside the expansion region of a seeded supersonic jet, at the temperature interval of 0.2K-0.7K [21]. The most known long-lived states, with lifetimes of up to several hours, are the circular Rydberg states, in which the outermost electron is localized to a planar circular orbit [22]. As the means of

 doi:10.20944/preprints202605.0506.v1

influencing the lifetimes, using external electric and magnetic fields have been implemented in one-electron Rydberg quasimolecules in [18]. The possibility of lifetime extension using quantum interference between molecular photoexcitation pathways connecting bound states and the dissociation continuum in Rydberg molecules has been shown in [23].

Along with meaningful lifetimes, the ability of Rydberg atoms to withstand intensive collisions during their interaction with the shock is the next requirement. The remarkable stability of Rydberg gas was indeed observed in collisions where the interaction did not lead to the transfer of electronic state of the atom to the state with another energy level or ionization continuum, but rather resulted in exchange of states between the colliding atoms. At very high excitation levels, the electron's orbit is extended very far from the core, and therefore collision with a Rydberg atom mainly occurs via interaction with its electron, rather than with the core. In this case the interaction proceeds in the form of electron scattering that results in the change of its angular momentum (l,m – mixing) but not the energy level of the electronic state. In a similar way, this happens when electric charges are present in the gas, in which collision of a Rydberg atom with a low-energy electron is also stabilizing. The process of charge transfer between a cation and a Rydberg atom in **c**ollisions, in which one Rydberg atom is replaced with another, is the efficient mechanism that ultimately does not affect Rydberg atom's population. Favorable outcomes of inelastic, state-changing collisions between different Rydberg state manifolds for Rb atoms in a low n-state ($20 > n > 40$) and ground-state atoms or electrons are confirmed in [24]. In short-lived Rydberg quasimolecular complexes, the oscillating electric field resulting from the charge exchange during collisions caused transitions within the Rydberg manifold. The stabilizing effects of dissociation or associative ionization of Rydberg states was also observed in [25] using high resolution spectroscopy in Rb. Inelastic and reactive collisions between Rydberg and ground state atoms considerably influenced lifetimes and quantum state of the scattered Rydberg atoms. This included redistribution over a wide range of their final states and the possibility of decay to the same angular momentum quantum numbers (l,m) state but for different principal quantum number n via l, m – mixing mechanism of electronic state exchange during electron scattering in the collision.

Thus the extensive evidence shows that the long lived Rydberg states are possible in a variety of laboratory or astrophysical environments. A great number of observations were also reported in relatively high temperature environments, such as gas discharges or stellar photospheres, i.e. under the conditions close to that achieved by compression in a shock wave. This assures that at the impact with the shock wave there will be no immediate quenching of Rydberg states. In terms of kinetics, at least for the relaxation time in the shocked gas, the high n-states fraction can be considered "frozen", i.e. treated as a fraction completely isolated from the low-n state (or ground-state) component.

II. The Model

The model describing interaction of a shock wave with a binary gas mix consisting of two components of the same sort of gas (Ar) will be based on the following assumptions. One of the components will be the high n-state Rydberg atoms, and another one is the ground-state atoms. Thus atoms of both components will have exactly the same mass, but their sizes will differ considerably. Even though, equivalently, the two components can represent any chemically non-reactive species of approximately the same mass but of unequal molecular size, in further description, as a convention, the atoms of larger size will be termed as Rydberg atoms and the smaller ones as those in the ground state. As it was mentioned above, the low-energy collisions are found to be supporting an enhanced stability of Rydberg atom population via l,m-mixing or charge exchange pathways, while high energy encounters likely result in Rydberg atom ionization. Because of this reason, to ensure the atom population stability in the mix, kinetical energies of atoms that are too high will be avoided by considering only weak shock waves. The choice of argon was drawn by the fact that in this gas the probabilities of the dipole-dipole transitions for high change in n are known to be low, while they are

 doi:10.20944/preprints202605.0506.v1

large for neighboring level transitions at high n-states. The strong coupling between high n,l,m-states and black body radiation results in a fairly low efficiency of radiative emission for high n-states. In argon atoms, the specific combination of probabilities represents the desired barrier in exchange between high-n and low n-states, resulting in isolation of high n states from low-n states or ionization continuum, and thus will be stabilizing for the mixture content.

The specific feature of the shock's impact on the gas mix of substantially different size atoms is the way the shock energy is transferred to each of the components. Because of large collisional cross section difference, the momentum transfer from the shock to the gas will be preferable via collisions between large atoms, and in a lesser degree - between large and small ones, rather than from small to small. Therefore in a substantially diluted gas, as a result of selective energy transfer, the flow of Rydberg atoms getting larger momentum from the shock will be higher than that for the ground-state atoms. In the process of diffusion between the components, Rydberg atoms will be pulled ahead of the smaller ones. As the result of re-distribution of the atom component concentrations, the shock front will attain the structure more complicated than just a single parameter distribution profile with continuous change of parameters across it.

Considering the problem in one dimension, the standard system of differential equations describing the mass, momentum, and energy conservation in the hypersonic flow across the shock will be used [1]. Accounting for the dissipation processes, the gas viscosity, heat conduction, and momentum exchange in elastic collisions, will be done as in [2,26]. Then the system of equations for the ground-state atom component takes the form

$$\frac{d}{dx}(\rho_1 u_1) = 0 \tag{1}$$

$$\rho_1 u_1 \frac{du_1}{dx} + \frac{dp_1}{dx} - \frac{d}{dx}\left(\frac{4}{3}\mu_1 \frac{du_1}{dx}\right) - \lambda_1 u_{1d} \frac{dT_1}{dx} = R_{12}(T_1, T_2, u_1, u_2, \sigma) \tag{2}$$

$$\frac{5}{2}\frac{d}{dx}(p_1 u_1) - \frac{d}{dx}\left(\frac{4}{3}\mu_1 u_1 \frac{du_1}{dx}\right) - \frac{d}{dx}\left(\lambda_1 \frac{dT_1}{dx}\right) + \frac{1}{2}\rho_1 u_1 \frac{du_1^2}{dx} = \Omega_{12}(T_1, T_2, u_1, u_2, \sigma) \tag{3}$$

and similarly, for Rydberg gas component,

$$\frac{d}{dx}(\rho_2 u_2) = 0 \tag{4}$$

$$\rho_2 u_2 \frac{du_2}{dx} + \frac{dp_2}{dx} - \frac{d}{dx}\left(\frac{4}{3}\mu_2 \frac{du_2}{dx}\right) - \lambda_2 u_{2d} \frac{dT_2}{dx} = R_{21}(T_1, T_2, u_1, u_2, \sigma) \tag{5}$$

$$\frac{5}{2}\frac{d}{dx}(p_2 u_2) - \frac{d}{dx}\left(\frac{4}{3}\mu_2 u_2 \frac{du_2}{dx}\right) - \frac{d}{dx}\left(\lambda_2 \frac{dT_2}{dx}\right) + \frac{1}{2}\rho_2 u_2 \frac{du_2^2}{dx} = \Omega_{21}(T_1, T_2, u_1, u_2, \sigma) \tag{6}$$

In the equations, the subscripts "1" and "2" refer to the ground- and Rydberg-state components accordingly, m is mass of atom, ρ is the mass density, p is the gas pressure, u is the flow speed in the reference frame when the shock is stopped, u_d is the diffusion speed in the term modeling the momentum fluxes generated by the temperature gradient, T is temperature, σ is the atomic cross section, μ is gas viscosity, λ is thermal conductivity, k is the Boltzmann constant, $T_{avg} = (T_1 + T_2)/2$, and x is the coordinate along the shock wave propagation direction.

The collision terms in the form of force $R_{21}(T_1, T_2, u_1, u_2, \sigma)$and energy exchange between the components $\Omega_{21}(T_1, T_2, u_1, u_2, \sigma)$ are given by the following expressions,

$$R_{12} = -\alpha_{12} n_1 n_2 \sqrt{T_{avg}}(u_1 - u_2),\ R_{21} = -R_{12} \tag{7}$$

$$\alpha_{12} = \frac{4}{3} m \sigma_{12} \sqrt{\frac{8k}{\pi m}} \tag{8}$$

$$\Omega_{12} = -R_{12} u_1 = -\alpha_{12} n_1 n_2 \sqrt{T_{avg}} u_1 (u_1 - u_2),\ \Omega_{21} = -R_{21} u_2 = -\alpha_{21} n_1 n_2 \sqrt{T_{avg}} u_2 (u_2 - u_1) \tag{9}$$

 doi:10.20944/preprints202605.0506.v1

The coefficients of viscosity in collisions between i - and j – components (i, j is 1 or 2)

$$\mu_{ij} = \frac{1}{\sigma_{ij}}\sqrt{\frac{mkT}{\pi}} \tag{10}$$

and for thermal conductivity

$$\lambda_{ij} = \frac{5}{2}C_V\mu_{ij} \tag{11}$$

quantify the two damping mechanisms critically depending on the atom size. Denoting the ground-state atom radius as r_1 and that for the Rydberg atom as r_2, and, given that the highly excited state orbit is very large, their ratio

$$\delta = r_2/r_1 \tag{12}$$

will always be larger or much larger than the unit.

The contribution to the viscosity μ_1 acting on the flow of the ground state atoms is due to collisions between the ground-state atoms themselves ($i = j = 1$), for which the collision cross section $\sigma_{11} = 2\pi r_1^2$, and between the ground- and Rydberg-state atoms ($i = 1$, $j = 2$) with the cross section $\sigma_{12} = \pi(r_1^2 + r_2^2) \approx \pi r_2^2$, so the total contribution to viscosity $\mu_1 = \mu_{11} + \mu_{12}$. Applying eq. (10) for the components μ_{11} and μ_{12}, we obtain

$$\mu_1 = \frac{1}{\pi r_2^2}\sqrt{\frac{mkT_1}{\pi}}\left(1 + \frac{\delta^2}{4}\right) \tag{13}$$

Similarly, for Rydberg atom component we add the contributions due to Rydberg-Rydberg and Rydberg-ground-state atom interactions, $\mu_2 = \mu_{22} + \mu_{12}$, for which, neglecting the term ~ $1/\delta^2$,

$$\mu_2 = \frac{1}{\pi r_2^2}\sqrt{\frac{mkT_2}{\pi}}\left(\frac{1}{4} + \frac{\delta}{1+\delta}\right) \tag{14}$$

Combining the system (1-6) with the ideal-gas equations of state $p_1 = n_1kT_1$, $p_2 = n_2kT_2$, and the density relations $\rho_1 = mn_1$, $\rho_2 = mn_2$, the corresponding variables in the equations can be converted to number densities $n_1(x)$ and $n_2(x)$. After division the momentum equation by m and the energy equation by (5/2)k, we obtain the system of six one-dimensional differential equations for six unknown functions $n_1 = n_1(x)$, $u_1 = u_1(x)$, $T_1 = T_1(x)$, $n_2 = n_2(x)$, $u_2 = u_2(x)$, and $T_2 = T_2(x)$, for the ground-state component

$$n_1\frac{du_1}{dx} + u_1\frac{dn_1}{dx} = 0 \tag{15}$$

$$n_1u_1\frac{du_1}{dx} + \frac{k}{m}\left(T_1\frac{dn_1}{dx} + n_1\frac{dT_1}{dx}\right) - \frac{4\mu_1}{3m}\frac{d^2u_1}{dx^2} - \lambda_1\frac{u_{1d}}{m}\frac{dT_1}{dx} = \frac{\alpha_{12}}{m}n_1n_2\sqrt{T_{avg}}(u_1 - u_2) \tag{16}$$

$$\frac{dn_1}{dx}T_1u_1 + \frac{dT_1}{dx}n_1u_1 + \frac{du_1}{dx}n_1T_1 - \frac{8}{15}\frac{\mu_1}{k}\left[\left(\frac{\partial u_1}{\partial x}\right)^2 + u_1\frac{d^2u_1}{dx^2}\right] - \frac{2\lambda_1}{5k}\frac{d^2T_1}{dx^2} + \frac{2m}{5k}n_1u_1^2\frac{\partial u_1}{\partial x} = \alpha_{21}n_1n_2\sqrt{T_{avg}}u_1(u_1 - u_2) \tag{17}$$

and for Rydberg atom component,

$$n_2\frac{du_2}{dx} + u_2\frac{dn_2}{dx} = 0 \tag{18}$$

$$n_2u_2\frac{du_2}{dx} + \frac{k}{m}\left(T_2\frac{dn_2}{dx} + n_2\frac{dT_2}{dx}\right) - \frac{4\mu_2}{3m}\frac{d^2u_2}{dx^2} - \lambda_2\frac{u_{2d}}{m}\frac{dT_2}{dx} = \frac{\alpha_{12}}{m}n_1n_2\sqrt{T_{avg}}(u_2 - u_1) \tag{19}$$

 doi:10.20944/preprints202605.0506.v1

$$\frac{dn_2}{dx}T_2u_2+\frac{dT_2}{dx}n_2u_2+\frac{du_2}{dx}n_2T_2-\frac{8}{15}\frac{\mu_2}{k}\left[\left(\frac{\partial u_2}{\partial x}\right)^2+u_2\frac{d^2u_2}{dx^2}\right]-\frac{2\lambda_2}{5k}\frac{d^2T_2}{dx^2}+\frac{2m}{5k}n_2u_2^2\frac{\partial u_2}{\partial x}$$
$$=\alpha_{21}n_1n_2\sqrt{T_{avg}}u_2(u_2-u_1) \quad (20)$$

The set (15-20) is the system of nonlinear ordinary differential equations that is solved as the initial value problem, in which all the boundary conditions are taken at a single point, $x = 0$. The equations are of the first degree relative to the flow velocities u_1 and u_2, and of the second degree for the densities n_1, n_2 and temperatures T_1 and T_2. Therefore, the boundary conditions are

$$u_1(x=0)=u_2(x=0)=u_0 \quad (21)$$

$$n_1(x=0)=n_{10},\ n_2(x=0)=n_{20} \quad (22)$$

$$\frac{dT_1}{dx}=0,\quad \frac{dT_2}{dx}=0,\quad \frac{dn_1}{dx}=0,\quad \frac{dn_2}{dx}=0 \quad (23)$$

in which the choice of the values u_0 and n_{20} will be discussed in the next paragraph below.

III. Results

To probe the size of the effect, the system of equations (15-20) was run numerically for the shock Mach number $M = 1.5$ in argon gas, at the initial temperature of 1500 K. It was assumed that before the shock comes, both gas components were in thermal equilibrium with each other, i.e. their temperatures were equal, $T_1(0) = T_2(0)$. Then the shock speed is $u_0 = V_{sw} = 1060\ m/s$ that, in the reference frame when the shock is stopped, is the speed of the flow incoming at the shock front. The component densities (22) in the undisturbed gas ahead of the shock n_{10} and n_{20} were taken in the range between 10^{17} and $10^{20}\ m^{-3}$. The numbers were chosen in the range of values at which Rydberg atoms are typically observed in gas discharges and afterglow plasma experiments, and that supported Rydberg atoms stability for the times of compression and after-shock relaxation. In accordance to experiments [19], typical plasma densities measured downstream of flowing afterglow are found in the range of 10^{15}–$10^{20}\ m^{-3}$. In low power glow discharges or in fast flowing afterglow, it is at the level of $10^{17}\ m^{-3}$ upstream and decaying to 10^{16} downstream. There is also a natural upper limit on the number density due to the presence of giant atoms in the same volume of gas.

In Figures 1-4, the results for densities $n_2(x)$ and $n_1(x)$ are presented for several values of the parameter $\delta = r_2/r_1$ between 2 and 20, and different fractional concentrations of Rydberg atoms in the mix. All the data is obtained for the undisturbed gas densities in the range of 10^{17}–$10^{20}\ m^{-3}$, $T_1(0) = T_2(0) = 1500$ K, and the shock Mach number $M = 1.5$. The transport coefficients μ and λ were taken constant assuming that in a weak shock wave the temperature change is not very large.

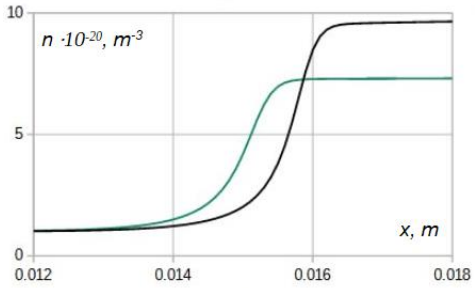

Figure 1. Density distribution profiles for the ground-state (black curve) and Rydberg atom (green) components for $\delta = 2$, at equal densities $n_1(0) = n_2(0) = 1.0\cdot10^{20}\ m^{-3}$, $T_1(0) = T_2(0) = 1500$ K, and $M = 1.5$.

In Figure 1, the density distribution profiles $n_1(x)$ and $n_2(x)$ are presented for the atom size ratio $\delta = 2$, at equal component's densities ahead of the shock $n_1(0) = n_2(0) = 1.0\cdot10^{20}\ m^{-3}$. As the graph shows, separately each profile represents a continuous distribution of the parameters across the shock front. The curve for Rydberg atom component (green) is shifted ahead of that for the ground state (black),

 doi:10.20944/preprints202605.0506.v1

with the shift value around $s = 0.7 \cdot 10^{-3}$ m. The relaxation lengths for each component determined as the widths of the transitional part of the profiles, are both close in value of around $3.0 \cdot 10^{-3}$ m. In accordance to the *Table I* presented in Appendix, at the gas and shock parameters of Figure 1, the mean free path length in the compressed gas for Rydberg atom component $L_R = 1.92 \cdot 10^{-3}$ m and that for the ground-state one $L_G = 6.07 \cdot 10^{-3}$ m. Thus the relaxation lengths and the splitting in Figure 1 are close in value and of the same order of magnitude as the mean free path lengths L_R and L_G.

The density profiles at larger atom size ratio $\delta = 5$ are presented in Figure 2, for the same gas conditions as in Figure 1 and for two different fractional concentrations of Rydberg atoms in the mix. In the graphs, two upper row profiles (black curves) are for the ground-state component, and the lower row profiles (green) are for Rydberg atoms. In column of graphs (***a***), the pair of profiles is obtained for the case of equal concentrations of the components, at the initial densities $n_1(0) = n_2(0) = 0.5 \cdot 10^{20}$ m^{-3}. In the case when Rydberg atoms prevail in the mix, $n_2(0) > n_1(0)$, the distributions are described with the pair of profiles in column (***b***) obtained at $n_2(0) = 0.4 \cdot 10^{20}$ m^{-3}, $n_1(0) = 0.1 \cdot 10^{20}$ m^{-3}.

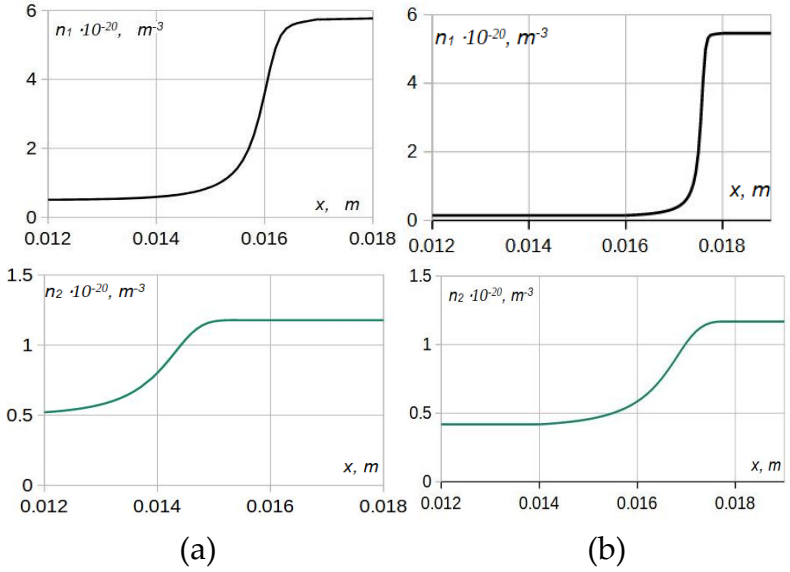

Figure 2. Density distribution profiles for the ground state (black curves) and Rydberg atom (green) components at $\delta = 5$, for two cases of Rydberg atom fractional concentration: Column ***a:*** $n_2(0) = n_1(0)$, Column ***b:*** $n_2(0) > n_1(0)$.

Comparing the graphs in each pair, it is seen that in both cases the green curve is shifted ahead of the black one. The shift value is around $s = 2\ 0 \cdot 10^{-3}$ m in case of $n_2 = n_1$, and $s = 3\ 0 \cdot 10^{-3}$ m for the case $n_2 > n_1$. In both cases the shifts and relaxation lengths are still close to each other in value, and they are of the same order of magnitude as the mean free path length L_R (Table I).

In Figure 3, the density profiles are obtained for $\delta = 10$, for two different fractional concentrations of the components. The pair of graphs in column (***a***) are for the case when Rydberg atoms are significantly less abundant than the ground state ones, at the undisturbed gas densities $n_2(0) = 0.5 \cdot 10^{19}$, $n_1(0) = 5.0 \cdot 10^{19}$, and the graphs in column (***b***) are for the case of equal concentrations of the components, $n_1(0) = n_2(0) = 0.2 \cdot 10^{19}$ m^{-3}.

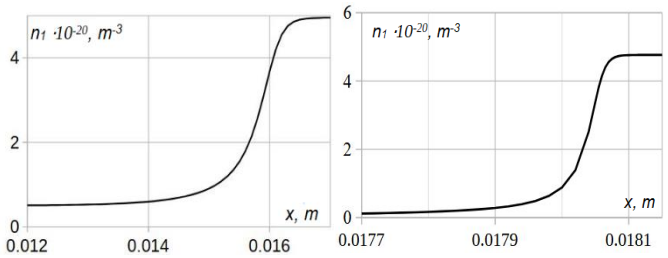

 doi:10.20944/preprints202605.0506.v1

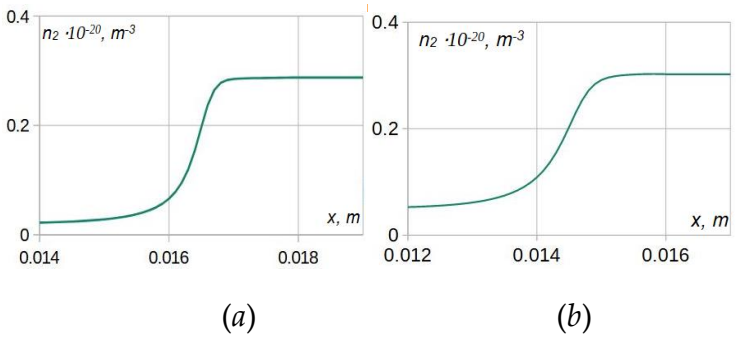

Figure 3. Density profiles for the ground-state (black curves) and Rydberg atom (green) components at δ = 10, for two cases of Rydberg atom fractional concentrations: graph ***a***, for $n_2(0) < n_1(0)$; graph ***b***, for $n_2(0) = n_1(0)$.

In the case of small fractional concentration of Rydberg atoms (1:10), the shift between the profiles $s = 1.0 \cdot 10^{-3}$ *m* (graphs ***a***), and the solution with similar characteristics was obtained for the concentration ratio 1:4. In case of equal component densities (graphs ***b***), the profile separation is slightly larger, around $s = 1.5 \cdot 10^{-3}$ *m*. In all cases, the relaxation lengths and the shifts are on the level of the mean free path length L_R.

At the next atom size ratio, δ = 20, the density profiles were obtained for the case $n_2(0) < n_1(0)$, with the initial densities $n_2(0) = 0.1 \cdot 10^{19}$ m^{-3}, $n_1(0) = 0.5 \cdot 10^{19}$ m^{-3} (Figure 4.). The shift between the profiles $s = 2.0 \cdot 10^{-3}$ *m*, and as in the previous cases, it is on the level of L_R. The relaxation length for Rydberg atom profile is around $2.0 \cdot 10^{-3}$ *m* and it tends to be wider than that for the ground-state atoms. The density jump for the ground-state component becomes noticeably higher than that for Rydberg atoms.

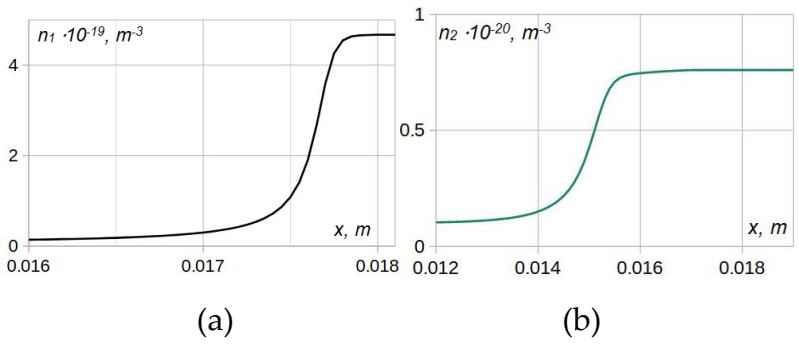

Figure 4. The density profiles for the ground-state (graph a) and Rydberg atom components (b) at δ = 20, for $n_2(0) < n_1(0)$.

The profiles with very close characteristics were obtained when running the system of equations for the case of equal component concentrations, $n_2(0) = n_1(0) = 0.2 \cdot 10^{19}$ m^{-3}.

Increasing the atom size ratio further, up to δ = 100 gives similar profiles (not presented) that follow the same tendency seen in the previous figures. At densities $n_2(0) = n_1(0) = 0.5 \cdot 10^{17}$ m^{-3}, the splitting is around $s = 3.0 \cdot 10^{-3}$ *m*, and it is close to the value of the relaxation length $L_R = 2.0 \cdot 10^{-3}$ *m* (Table I). The density jump across the shock for the ground-state component becomes significantly larger than that for Rydberg atoms, increasing approximately as ~ δ^3, and the relaxation length for this component visibly shortens, all in proportion to the density jump value.

Thus for all atom size ratios, fractional component concentrations, and the gas densities considered here, there is a clear shift between the profiles on the order of a mean free path L_R. The full compression of the larger size component occurs earlier than for the smaller one, thus forming two layers, each for one sort of atoms. The obtained distribution suggests splitting of the shock front in two, in which the first front formed by larger atoms is located ahead of the second one formed by smaller atoms. The size of the front splitting did not show direct dependence on the atom size ratio

 doi:10.20944/preprints202605.0506.v1

or the gas density. Instead, it is rather scaled with the mean free path L_R as a single parameter that combines both, the atom size and the density factors.

IV. Conclusions and Discussion

The study of weak shock waves in a monatomic gas mix with Rydberg atoms showed that the shock front attains specific structure characterized by the front splitting. The phenomenon is due to atomic size difference that works through variation in energy transfer to the gas components. The density profiles were obtained by solving the system of hydrodynamic equations in which the viscosity, thermal conduction, and momentum/energy exchange are the terms that are dependent on collision cross section, and therefore are those contributing to each component's dynamics differently. At the time of the shock strike, the selective transfer of momentum to the gas components generates the flows that are dependent on the atom size. The diffusion between two components induced by the shock leads to their concentration re-distribution thus forming the shock structure more complex than just a conventional transitional profile with continuous distribution of parameters. The results were obtained in the interval of gas parameters typical for the environments known to produce and sustain enough long-lived Rydberg atoms. In the calculations, the fractional concentration of Rydberg atoms in the mix was varied between less, equal, and larger than that for the ground state component, thus covering a wide range of the atom's abundances.

For each component separately, the density distribution in the transitional layer across the shock represented a simple exponential profile with a smooth change of the parameter. As the distinct feature, a clear shift between the profiles was present for all considered values of the atom size ratio δ, gas densities, and the fractional component concentrations, thus implying the species separation at the shock front. The profiles for Rydberg atoms were always ahead of that for the ground-state ones, suggesting that at the moment of the shock strike larger atoms are pulled ahead of the rest. Therefore, as the shock of initially plain structure enters the gas mix, its front splits into two, with larger atoms being concentrated ahead of the smaller ones. Significant lag between the profiles also shows that the full compression of Rydberg atom gas is achieved earlier than that for the ground-state component. For moderate atom size ratios, the splitting and the component's relaxation lengths were found close in value, all being on the order of mean free path length for Rydberg atoms L_R. As the size ratio increases, the small atom relaxation length shortens because of significant compression of this component. Thus the main shock structure characteristics are determined by Rydberg atom component, the one most quickly reacting to disturbance by the shock and during the relaxation time. The time scale $\tau = L_R/u_0$ at which the transitional layer forms is relatively short because of equal atomic masses for the components, for which the energy exchange during the collisions is highly efficient. Therefore, among the factors that can affect the component separation size, the immediate ones are those controlling the mean free path length. As such, the reduced gas densities featuring longer mean free path, or using molecular gases in which the excitation of additional degrees of freedom will delay the relaxation, are the ways to make the separation more observable.

The physical mechanism of the effect is determined by the selective way of the energy transfer from the shock to the gas components that is dependent on their atom size. With substantial difference in collisional cross section for the two components, momentum transfer from the shock will proceed preferably via collisions between large atoms (and in lesser degree between large and small), rather than from small to small. Therefore, in substantially diluted gas, the flow of larger atoms will be higher than that for the smaller ones. In the process of diffusion between the components, larger size atoms are pulled ahead of the smaller ones. It immediately follows then that diversion of the interaction to mostly large-to-large atoms at the shock front leaves the small size component essentially out of participation. In this situation, their role will be mostly reduced to the energy damping and mediating the relaxation that eventually fades the component separation away after the shock is gone. Then, with the small atom component essentially switched off from the interaction, the shock wave will mostly propagate through the gas of larger atoms. This explains the

 doi:10.20944/preprints202605.0506.v1

scale of the front splitting that is on the order of larger atom mean free path, not the smaller one, and this tendency increases with the atom size difference.

The atom size effect described here is somewhat similar to the effect of different atomic masses, in which lighter particles play a role analogous to the larger size atoms. The key difference between them is the relaxation timing, which is longer in case of considerable mass difference because of less efficient energy transfer in collisions. The relaxation is delayed because in this case many, up to thousands, collisions are required to bring the gas state to new equilibrium.

In analyzing the technical problems encountered in solving the system of equations, the following should be mentioned. With only viscosity and collision terms included in the equations, the solutions developed singularities that typically occurred at later points in the profiles. In all cases however, clearly distinct shifts between front parts of the profiles were still present, with larger atom profiles being ahead. The singularities mostly featured the ground-state atom profiles while those for Rydberg atoms could be finite, and applying a number of sophisticated packages available within the software could not fix the problem. Adding two terms, the thermal conduction terms to the energy equation and the term modeled the temperature gradient generating momentum fluxes, however removed the singularities instantly. Similar situation was mentioned in the study of diffusive charge separation effects in [27] when using a simplified form of the Navier-Stokes equations. Thus the contribution of thermal gradients in the form of thermal conduction and additional, diffusion induced momentum transfer, appear among the vital mechanisms shaping the shock structure.

The findings can be of interest in the research areas such as hypersonic plasma dynamics and astrophysics where the key processes are predominantly mediated by collisions, as for ex. in the supernovae atmospheres in the presence of rapid expansion, in which the expelled material at a high speed creates shock waves that interact with surrounding circumstellar material. Considering ground-state atoms as perturbers, collisions with them will modify the quantum state of Rydberg atoms that include mixing with the ionization continuum. This naturally limits the application range with Rydberg atom stability necessary to endure the compression in a shock wave and collisions during the relaxations. In astrophysics and cosmology environments, the radiation produced during the transition between closely spaced Rydberg states is routinely used for identification of the chemical composition and physical conditions of the stars, and for understanding the evolution in the photosphere [28,29]. As their specific property, the extremely long Rydberg atom lifetimes are employed for probing dynamical processes that proceed on a fast time scale. Other media with applicable properties are also confirmed in white dwarf photosphere, weakly ionized regions within active galactic nuclei, and in the solar photosphere.

Rydberg matter, an exotic phase of matter formed by Rydberg atoms in astrophysical media, exists in the form of long-lived hexagonal, planar clusters, and it is similar to dusty plasmas with small clusters in a gas [30,31]. Significantly long lifetimes of clusters is the consequence of impeded de-excitation by exchange-correlation effects in the non-uniform electron liquid formed on condensation by the collective valence electron. Their stability combined with the possibility for large size clusters, can make it another area of interest. In laboratory plasmas, Rydberg molecular ions are other applicable candidates to study the effect under the conditions of delayed molecular relaxation. During collisions of the ions with neutral particles, transiently populated Rydberg states can influence scattering probabilities and relaxation pathways, thus enhancing or impeding particular chemical reactions. The reactions can be laser controlled by steering the ion toward specific electronic or nuclei quantum states, as for ex. was done in the study of purification of mixtures of enantiomers and chiral molecules [32].

Appendix

Presented in *Table* 1, the mean free path lengths L_R (j = 2) for Rydberg atoms, and L_G (j = 1) for ground-state atoms are calculated in compressed gas, for several values of the parameter δ and different undisturbed gas densities $n_j(0)$,

 doi:10.20944/preprints202605.0506.v1

$$L_j = \left(\sqrt{2} n_j \sigma_j\right)^{-1}, \tag{24}$$

In each cell of the table, upper value is the mean free path L_R, and the lower number is for L_G.

Table I. Mean free path lengths in the compressed gas for Rydberg and ground-state atom components in meters, in the form L_R/ L_G, for different undisturbed gas densities $n_j(0)$ and several values of the parameter δ.

$n(0)\cdot 10^{-20}\ m^{-3}$	δ = 2	δ = 5	δ = 10	δ = 20	δ = 100
1.0	$1.92\cdot10^{-3}$ $6.07\cdot10^{-3}$				
0.50		$1.94\cdot10^{-3}$ $1.06\cdot10^{-2}$	– $5.83\cdot10^{-2}$		
0.10		$9.72\cdot10^{-3}$ $5.30\cdot10^{-2}$			
0.05			$9.72\cdot10^{-3}$ –	– $5.83\cdot10^{-2}$	
0.02			$9.72\cdot10^{-3}$ $5.83\cdot10^{-2}$		
0.01				$9.72\cdot10^{-3}$ –	
0.00005					$9.72\cdot10^{-3}$ $6.48\cdot10^{-2}$

References

1. Ya. B. Zel'dovich, Yu. P. Raizer, *Physics of Shock waves and High-Temperature Hydrodynamic Phenomena*, Academic Press, New York and London, 1967.
2. S. I. Braginski, *Transport Processes in a Plasma,* Reviews of Plasma Physics, Vol. 1, 1965.
3. G.B. Whitham, *On the propagation of weak shock waves*, Journal of Fluid Mechanics, 1, pp. 290-318.
4. G. A. Bird, *The motion of a shock-wave through a region of non-uniform density*, Journal of Fluid Mechanics, September 1961, DOI:10.1017/S0022112061000457.
5. Katz E. J. *A ray theory for wave propagation in a non-uniform medium,* Journal of Fluid Mechanics, 16(3), pp. 343-356 (1963). doi:10.1017/S0022112063000811.
6. R. F. Chisnell and M. M. Yousaf, *The effect of the overtaking disturbance on a shock wave moving in a non-uniform medium*, Journal of Fluid Mechanics, Vol. 120, pp. 523–533 (1982).
7. F. Obermeier, *On the propagation of weak and moderately strong, curved shock waves*, J. Fluid Mech., Vol. 129, pp.123-136 (1982)
8. A. Markhotok, *A shock wave instability induced on a periodically disturbed interface*, IEEE Transactions on Plasma Science **46**, Issue 8, pp. 2821 – 2830 (2018), DOI: 10.1109/TPS.2018.2848597.
9. A. Markhotok, *Shock–Discharge Interaction Model Extended into the Third Dimension*, *Plasma* 2024, **7**(2), 355-365; https://doi.org/10.3390/plasma7020020.
10. A. Markhotok, *The Post-Shock Nonequilibrium Relaxation in a Hypersonic Plasma Flow Involving Reflection off a Thermal Discontinuity*, Plasma, Volume 6, Issue 1, 181-19 (2023).
11. T. Galladner, *Rydberg Atoms*, Cambridge Univ. Press, 1994.
12. C. A. Bertulani, T. Frederico, M. S. Hussein, *On the existence of Rydberg nuclear molecules*, Physics Letters B, Volume 774, pp. 247-251 (2017).
13. M. Y. Ivanov, A. Stolow, *Coherent control of high-n Rydberg lifetimes using wavepacket technology,* Chemical Physics Letters 265, pp. 231-238 (1997).
14. A. Wojciechowska, M. Tomza, and M. T. Eiles, *Ultralong-range Rydberg molecules of Hg atoms*, Phys. Rev. A (111), 042816 (2025), DOI: https://doi.org/10.1103/PhysRevA.111.042816

 doi:10.20944/preprints202605.0506.v1

15. S. Markson, S. T. Rittenhouse, R. Schmidt, J. P. Shaffer, and H. R. Sadeghpour, *Theory of Ultralong-Range Rydberg Molecule Formation Incorporating Spin-Dependent Relativistic Effects: Cs(6s)–Cs(np) as Case Study*, Chem. Phys. Chem., 17, pgs. 1 – 10 (2016) DOI: 10.1002/cphc.201600932.
16. C. Fey, F., Hummel, & P. Schmelcher, *Ultralong-range Rydberg molecules*, Molecular Physics, 118(2) (2020). https://doi.org/10.1080/00268976.2019.1679401
17. N. Schlossberger, T. McDonald, N. Prajapati, and C. L. Holloway, *Rydberg atom reception of a handheld UHF frequency-modulated two-way radio*, Phys. Rev. Appl. 25, 024031 (2026).
18. A. E. Lilley, and P. Palmer, *Tables of Radio-Frequency Recombination Lines*, Astrophysical Journal Supplement, vol. 16, p.143 (1968).
19. R. S. Mason, P. D. Miller, I. P. Mortimer, D. J. Mitchell and N. A. Dash, *Positive-column plasma studied by fast-flow glow discharge mass spectrometry: Could it be a Rydberg gas?*, Phys. Rev. E, Volume 68, Issue 1, 68, 016408 (2003).
20. S. M. Tarr, J. A. Schiavone, R. S. Freund, *Long-lived high-Rydberg molecules formed by electron impact: H2, D2, N2, and CO*, J. Chem. Phys. 74, 2869–2878 (1981) https://doi.org/10.1063/1.441406.
21. G. Jingwei, V. Mervash, R. Mikko, M.-D. Klaus, *Some properties of a long lifetime strongly-coupled molecular plasma produced by high Rydberg excitation of nitric oxide in a supersonic free jet*, preprint arXiv:0904.2280, Pub Date: April 2009 DOI: 10.48550/arXiv.0904.2280
22. E. Pultinevicius, A. Götzelmann, F. Thielemann, C. Hölzl, F. Meinert, *Long-lived giant circular Rydberg atoms at room temperature*, arXiv:2510.27471.
23. A. García-Vela, *Quantum Control of Resonance Lifetimes in Molecular Photodissociation with Intense Laser Fields*, Journal of Chemical Theory and Computation, Vol 21/Issue 4, Dynamics (2025).
24. P. Geppert, M. Althon, D. Fichtner, and H. Ott, *Diffusive-like distribution instate-changing collisions between Rydberg atoms and ground state atoms*, Nature Communications, Volume 12, Article number: 3900 (2021).
25. M. S. Dimitrievic, V. A. Sreckovic, A. A. Zalam, *Dynamic instability of Ry atomic complexes*, Atoms 7, 22 (2019).
26. S. Chapman and T. G. Cowling, *The mathematical Theory of non-uniform gases*, 3rd Edition, Cambridge Univ. Press, 3rd Ed., 1970.
27. H. K. Sen, O. W. Greenberg, and Y. M. Treve, *Diffusion effects on the shock structure in a plasma*, Planetary and Space Science, V. 4, pp. 358-373 (1961).
28. Y. Osorio, P. S. Barklem, K. Lind, A. K. Belyaev, A. Spielfiedel, M. Guitou6 and N. Feautrier, *Mg line formation in late-type stellar atmospheres*,Astronomy and Astrophysics, Volume 579, Article Number A53 (2015). https://doi.org/10.1051/0004-6361/201525846.
29. Y. N. Gnedin, A. A. Mihajlov, L. M. Ignjatović, N. M. Sakan, V. A. Srećković, M. Yu. Zakharov, N. N. Bezuglov, A. N. Klycharev. *Rydberg atoms in astrophysics*, New Astronomy Reviews, Volume 53, Issues 7–10, pp. 259-265 (2009).
30. J. Wang, and L. Holmlid, *Rydberg Matter clusters of hydrogen with well-defined kinetic energy release observed by neutral time-of-flight*, Chemical Physics. 277(2): 201 (2002). doi:10.1016/S0301-0104(02)00303-8.
31. E. A. Manykin, M. I. Ozhovan, P. P. Poluéktov, *Transition of an excited gas to a metallic state*, Sov. Phys. Tech. Phys. Lett. 6: 95 (1980).
32. P. Kral, I. Thanopulos, and M. Shapiro, *Colloquium: Coherently controlled adiabatic passage*, Rev. Mod. Phys. 79, 53 (2007), DOI: https://doi.org/10.1103/RevModPhys.79.53